LATTICE DYNAMICS
AND PHASE TRANSITIONS

Heat Capacity, Structure, and p–T Phase Diagram of Elpasolite $(NH_4)_2KMoO_3F_3$

I. N. Flerov[a], M. V. Gorev[a], V. D. Fokina[a], A. F. Bovina[a], M. S. Molokeev[a], E. I. Pogorel'tsev[a], and N. M. Laptash[b]

[a] *Kirensky Institute of Physics, Siberian Division, Russian Academy of Sciences,*
Akademgorodok, Krasnoyarsk, 660036 Russia
e-mail: flerov@iph.krasn.ru

[b] *Institute of Chemistry, Far Eastern Division, Russian Academy of Sciences,*
pr. Stoletiya Vladivostoka 159, Vladivostok, 690022 Russia

Received April 10, 2006

Abstract—Thermophysical and structural studies of an $(NH_4)_2KMoO_3F_3$ crystal show that this crystal belongs to the family of elpasolites (space group $Fm\bar{3}m$) and undergoes an order–disorder phase transition at $T_0 =$ 241.5 K. Under hydrostatic pressure, this phase transition splits into two consecutive transitions at the tricritical point with parameters $T_{tr} = 232.5$ K and $p_{tr} = 0.21$ GPa. It was found that anomalous hysteresis and relaxation phenomena accompany the transitions from the cubic to both distorted phases. The results are analyzed taking into account the data on the phase transition in the related elpasolite $(NH_4)_2KWO_3F_3$.

1. INTRODUCTION

Oxyfluorides with the general formula $A_2A'MO_3F_3$ (A, A' = K, Rb, Cs; M = Mo, W) differ from "pure" oxides and fluorides in that they have a lower (noncubic) symmetry of the six-coordinated anion (quasi-octahedron), which, according to cis- and trans-configurations of ligands, can be either trigonal (C_{3v}) or orthorhombic (C_{2v}) symmetry. In spite of this fact, the symmetry of the crystal lattice of oxyfluorides remains cubic with space group $Fm\bar{3}m$ ($Z = 4$) because of statistical disordering of the $F(O)$ atoms [1].

The compounds containing spherical cations $A = A'$ (cryolites) undergo a sequence of two (ferroelectric and/or ferroelastic) phase transitions. The size of the central atom M in the octahedron has a significant effect on the temperature (T_1) of the ferroelectric transition from the cubic phase. In compounds with M = Mo, the higher temperature transition occurs at a temperature T_1 that is 50–70 K higher than that in tungstates. The influence of the central atom size on T_2 is far weaker. The changes in entropy (ΔS) are rather small for both transitions, and only for $Cs_3WO_3F_3$ are they close to $R\ln 2$. According to the values of ΔS, it can be concluded that there is no disordering of any structural elements in the cubic structure of the cryolites studied. Therefore, the phase transitions are believed to be related to atomic displacements, which result simultaneously in spontaneous polarization and spontaneous deformation. Judging from the spontaneous polarization behavior and

from the fact that thermal effects have been easily detected by a low-sensitive DTA technique [1], the phase transitions in cryolites are most probably of the first order.

Substitution of atomic cations by a tetrahedral ammonium ion simultaneously in two different crystallographic positions, namely, in the center of an octahedron ($4b$) and in an interoctahedral void ($8c$), leads to a significant decrease in the temperature of instability of the cubic phase and to a narrowing of the range of existence of the intermediate distorted phase. For example, the transition temperatures in the fluorine-oxygen cryolite $(NH_4)_3WO_3F_3$ are very close to each other: $T_1 =$ 200.1 K and $T_2 = 198.5$ K [2]. The observed significant increase in the entropy of the phase transitions ($\Sigma\Delta S_i \approx$ $R\ln 8$) as compared to the corresponding values in compounds containing atomic cations suggests that the transitions are typical order–disorder transitions.

If positions $4b$ and $8c$ are occupied by different types of cations ($A \neq A'$), the $A_2A'MO_3F_3$ compounds have an elpasolite structure. In this case, the pattern of the phase transitions is different. The sequence of two transitions remains only in the $Rb_2KMoO_3F_3$ compound, whereas in oxyfluorides $Rb_2KWO_3F_3$, $Cs_2RbMoO_3F_3$, and $Cs_2RbWo_3F_3$ only one phase transition occurs [1]. The elpasolites $Cs_2KMO_3F_3$ (M = Mo, W) remain cubic down to 80 K. There was no information on the thermodynamic parameters of elpasolites, except on the phase transition temperatures. Therefore,
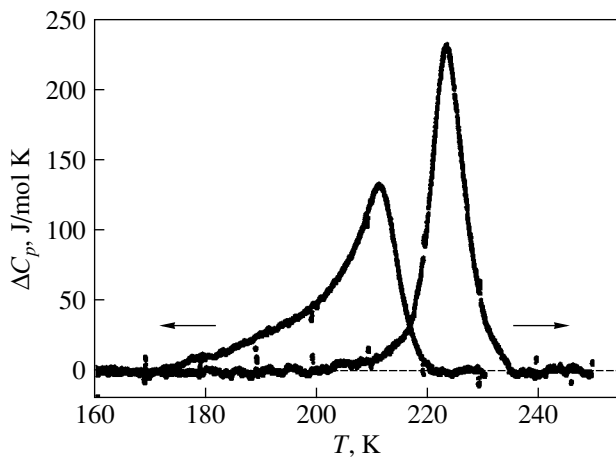
Fig. 1. Temperature dependence of the heat capacity of the compound $(NH_4)_2KMoO_3F_3$ obtained by DSM in heating and cooling regimes.

it was, for example, impossible to find a correlation between the entropy and size of spherical cations in positions $4b$ and $8c$. On the other hand, ferroelectricity was found below T_1 in some of these structures [1].

The effect of the type of cation in position $8c$ on the phase transitions in the elpasolite $(NH_4)_2KWO_3F_3$ was studied in [3]. It has been established that this compound has a cubic elpasolite structure at room temperature; this structure becomes unstable only at a temperature $T_0 = 235.4$ K, which is lower than, for example, that in the $Rb_2KWO_3F_3$ compound ($T_1 = 291$ K) [1]. The ferroelastic phase transition in ammonium elpasolite is of the second order and is accompanied by a relatively small change in entropy ($\sim R\ln 2$). An analysis of electron density distribution maps of atoms F(O) has shown that vibrations of the ligands are characterized by a pronounced anisotropy, as in cryolite $(NH_4)_3WO_3F_3$. However, in the latter compound, the thermal parameters of atoms F(O) are significantly higher. In [3], information on the enthalpy and entropy of the phase transition was obtained for the first time, as well as information on the $p–T$ phase diagram for fluorine–oxygen elpasolites.

The difference between the ionic radii of molybdenum (0.60 Å) and tungsten (0.59 Å) is very small, and, at first glance, the significant difference between the transition temperatures in fluorine-oxygen cryolites with an elpasolite structure containing these atoms seems unusual. In related fluorides containing atomic, molecular, or mixed cations, the difference in the transition temperatures corresponds to a more significant difference in the ionic radii of Al–In atoms located in the $4a$ position (about 0.2 Å) [4, 5]. On the other hand, according to the authors of [6], the temperature of the transition from the cubic phase in oxyfluorides containing atomic cations can be influenced by an increase in the covalency of the M–O bond caused by the substitu-

tion W $\longrightarrow$ Mo. It remains yet unknown how this substitution influences the crystals containing an ammonium cation. The thermodynamic properties, structure, and $p–T$ phase diagram of the elpasolite $(NH_4)_2KMoO_3F_3$ are studied in this work to solve this problem.

2. DETECTION OF PHASE TRANSITIONS

The octahedral crystals $(NH_4)_2KMoO_3F_3$ were obtained from a molybdenum–ammonium water solution with excess HF through addition of a potassium fluoride solution. The stoichiometry of the compound was tested by chemical analysis. The experimentally established and calculated (in parentheses) elemental compositions are as follows (in mass %): 13.0 (13.05) NH_4, 13.8 (14.17) K, 34.9 (34.76) Mo, and 20.3 (20.65) F. The ammonium content was determined by the Kyeldal method, the potassium and molybdenum contents were determined by the atomic-absorption method, and the fluorine content was determined by distillation in the form of H_2SiF_6 followed by titration in nitric-acid thorium.

At the first stage, the sample was studied on an x-ray diffractometer DRON-2. At room temperature, the compound studied has a cubic symmetry with space group $Fm\bar{3}m$; i.e., as expected, it belongs to the family of elpasolites. The lattice parameter of $(NH_4)_2KMoO_3F_3$ ($a_0 = 9.013$ Å) is close to that of the tungsten-containing analog ($a_0 = 8.958$ Å), because the Mo and W ionic radii are close to each other.

The thermal stability of the cubic structure was analyzed by heat capacity measurements of a powder sample on a DSM-2M differential scanning microcalorimeter. The temperature scanning rate was 8 K/min. The 0.16-g sample was placed in an aluminum container.

A heat capacity anomaly in the form of a sharp peak with a maximum at $T_0 = 223$ K was observed during heating in the temperature range 120–270 K. The measured excess heat capacity ΔC_p is shown in Fig. 1; this quantity is determined as the difference between the total molar heat capacity of the compound and its lattice component. The significant hysteresis in the transition temperature ($\delta T_0 \approx 12$ K) found during the thermal cycling experiments confirms that the transition is of the first order.

Integration of the function $\Delta C_p(T)$ gives the value of the enthalpy related to the phase transition $\Delta H = 1800 \pm 200$ J/mol.

The structural nature of the phase transition was confirmed by an analysis of the x-ray diffraction pattern of the low-temperature phase $(NH_4)_2KMoO_3F_3$ at 130 K. The structural model used was based on a pseudotetragonal unit cell, because the basic reflections of the distorted phase corresponded to this symmetry. Figure 2a shows the typical profiles of the (400) reflection in the initial cubic and the distorted phases. As is

seen from Fig. 2a, the structural distortion is manifested in a significant splitting of the reflection, which suggests a lowering of the symmetry as a result of the phase transition. Figure 2b shows the temperature dependence of the pseudotetragonal unit cell parameters with the ratios $a_{tetr} \approx a_{cub}/\sqrt{2}$ and $c_{tetr} \approx a_{cub}$. The jumps in the parameters detected at the transition point confirm that the structural transition is of the first order.

3. HEAT CAPACITY MEASUREMENTS

Detailed measurements of the temperature dependence of the heat capacity of $(NH_4)_2KMoO_3F_3$ were performed under conditions much closer to equilibrium by using an adiabatic calorimeter. The 0.59-g sample studied was hermetically sealed in an indium container in a helium atmosphere. The measurements were performed in discrete ($\Delta T = 2.5$–4.0 K) and continuous ($dT/dt = 0.18$ K/min) heating regimes. The vicinity of the phase transition was studied using quasi-static thermograms with average heating and cooling rates $|dT/dt| \approx 0.04$ K/min.

The results of two runs of heat capacity measurements performed in continuous heating regimes at the same rate are shown in Fig. 3. At this stage, we were interested only in measuring the transition temperature; therefore, the total heat capacity of the sample and the accessories is shown in the diagram. The heat capacity was found to exhibit an anomalous behavior caused by the phase transition. In numerous repeated experiments, it was established that the temperature of the anomaly maximum depends significantly on the prehistory of a specific run of measurements. If the measurements are performed immediately after cooling of a sample held for several hours at room temperature, then the transition takes place at $\approx$239 K. However, if a sample was held for a long time at $\approx$77 K before measurements, the transition temperature increases gradually from one run of measurements to the next. For example, we detected an anomaly at 243 K in one of the cycles. In this case, the peak in the heat capacity is wider and its maximum value is lower (Fig. 3). The area under the peak (corresponding to the enthalpy of the phase transition) remains unchanged during thermal cycling to within the accuracy of its determination. It should be noted that, in the experiments with a lower heating rate realized in the quasi-static thermographic regime, the same ageing effects in the sample were observed.

Adiabatic calorimeters are specific in that they allow measurements of the heat capacity of a sample to be performed over a wide temperature range in the heating regime only. Therefore, the heat capacity in the cooling regime was measured only using the quasi-static thermogram technique (Fig. 3). It should be noted that the temperature of the maximum heat capacity corresponding to the temperature of the structural transition
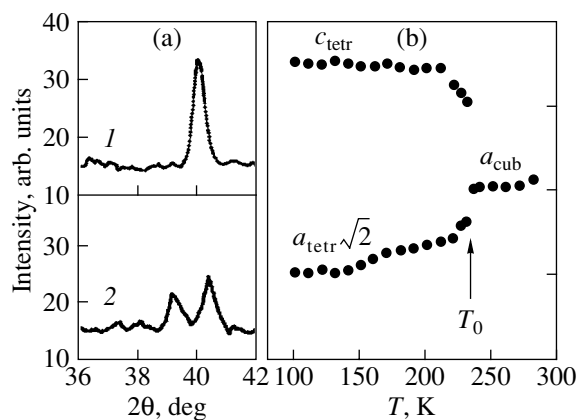

Fig. 2. Results of x-ray studies of $(NH_4)_2KMoO_3F_3$: (a) the (400) reflection at (*1*) 293 and (*2*) 123 K and (b) the temperature dependence of the unit cell parameters.
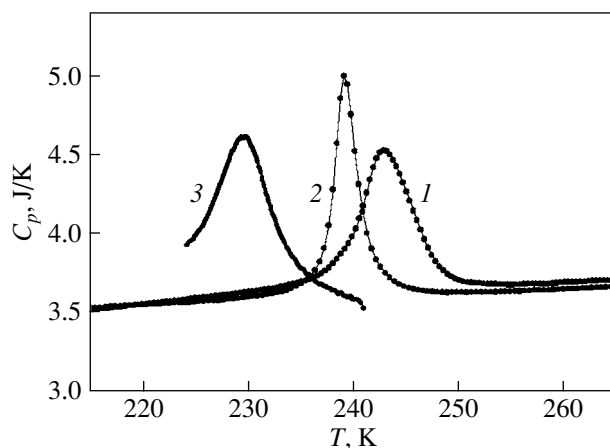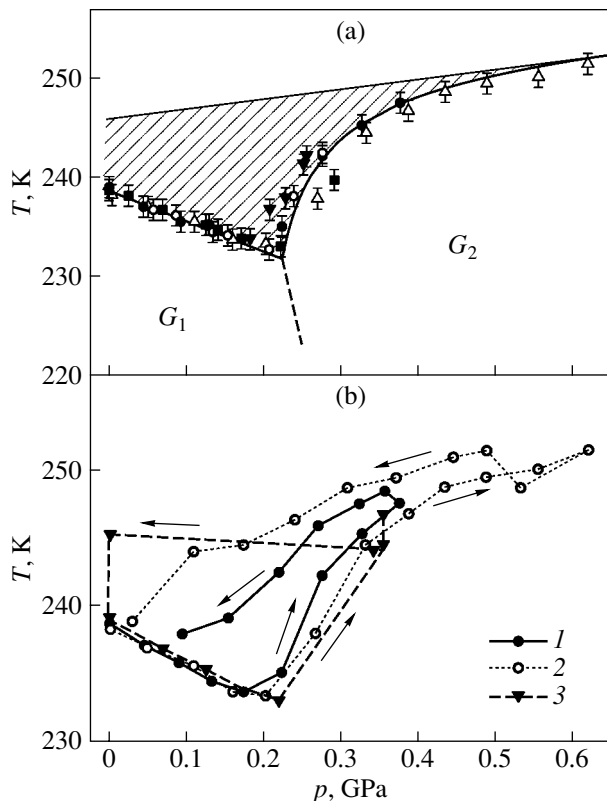

Fig. 3. Temperature dependence of the heat capacity of the "accessories + sample" system near a phase transition measured (*1*) after prolonged holding of the sample at room temperature, (*2*) after repeated heat cycling, and (*3*) in the regime of thermographic cooling.

231.5 ± 0.5 K was almost entirely independent of the prehistory of the measurements.

An analysis of the experimental data on the $(NH_4)_2KMoO_3F_3$ heat capacity measured repeatedly on an adiabatic calorimeter and differential calorimeters at various temperature rates indicates that the equilibrium phase transition is observed in the measurements performed at a rate $dT/dt \approx 0.04$ K/min immediately after the sample was held for 10–15 h at room temperature. The temperature $T_0 = 241.54 \pm 0.04$ K corresponding to the maximum of the heat capacity peak was considered the temperature of an equilibrium structural transition. In this case, the thermal hysteresis is $\delta T_0 = 10.0 \pm 0.5$ K, which is comparable to the value obtained in the DSM measurements.
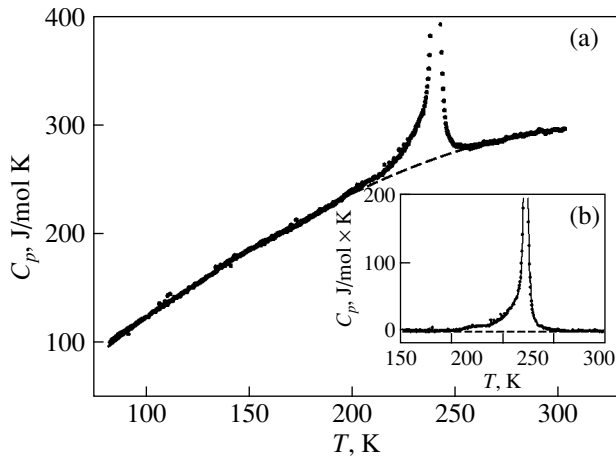
Fig. 4. Temperature dependence of (a) the heat capacity and (b) excess heat capacity of oxyfluoride $(NH_4)_2KMoO_3F_3$ measured over a wide temperature range.

Fig. 5. (a) p–T phase diagram of oxyfluoride $(NH_4)_2KMoO_3F_3$ and (b) the results of studying the hysteresis phenomena in the region of equilibrium of the cubic and distorted phases.

Figure 4a shows the temperature dependence of the molar heat capacity calculated from the heat capacity values measured over a wide temperature range. The dashed line corresponds to the regular heat capacity,

which was obtained by fitting the function $C_p(T)$ to a polynomial beyond the phase transition region.

The behavior of the excess heat capacity due to the phase transition (Fig. 4b) suggests that the anomalous contribution exists in a rather wide temperature range both below and above the phase transition temperature (down to $T_0 - 60$ K and up to $T_0 + 20$ K). The calculated changes in enthalpy and entropy are $\Delta H_0 = 3100 \pm 150$ J/mol and $\Delta S_0 = 13.0 \pm 0.7$ J/mol K, respectively.

Since the observed phase transition is of the first order, it is interesting to determine the latent heat (the jump in enthalpy). Latent heat absorption was detected during heating of a sample in the quasi-static thermographic regime in the interval $T_0 \pm 0.3$ K, and its value was found to be $\delta H_0 = 2160 \pm 220$ J/mol. The corresponding jump in entropy is $\delta S_0 = \delta H_0/T_0 = 8.9 \pm 0.9$ J/mol K.

4. p–T PHASE DIAGRAM

The p–T phase diagram of the elpasolite $(NH_4)_2KMoO_3F_3$ was studied on a ~0.1-g sample by the DTA technique under pressure. The method used in these studies is described in [2]. The phase equilibrium lines in the p–T diagram (Fig. 5a) were determined by increasing and decreasing the hydrostatic pressure. The line corresponding to the $Fm\bar{3}m \longrightarrow G_1$ phase transition (which was observed at atmospheric pressure) remains linear with a slope $dT/dp = -28 \pm 3$ K/GPa up to the point with parameters $T_{tr} = 232.5$ K and $p_{tr} = 0.21$ GPa. The results were reproduced many times under increasing and decreasing pressure. The abrupt break in the slope of the phase transition curves at this point is accompanied by a change in the sign of dT/dp and confirms unambiguously that this is a tricritical point with the thermodynamic parameters indicated above.

The transition line between two distorted phases G_1 and G_2 was not observed in the experiments. There could be two reasons for this. First, the areas under the DTA peaks corresponding to the enthalpies of the transitions from the cubic to G_1 and G_2 phases remained almost unchanged to within the limits of accuracy throughout the pressure range studied. Therefore, the change in enthalpy (and entropy) caused by the $G_1 \longrightarrow G_2$ transition is small and cannot be detected by the DTA technique. It is possible that this transition is of the displacement type due to its small entropy. Second, the $G_1 \longrightarrow G_2$ phase transition line can be characterized by an anomalously high derivative dT/dp, which also significantly decreases the probability of detecting the phase transition. The phase equilibrium line shown in the p–T diagram is determined by analyzing the Clapeyron–Clausius equation.

The nonlinear curve between the $Fm\bar{3}m$ and G_2 phases is characterized by an anomalously high initial

Table 1. Parameters of data collection and structural refinement of the compound $(NH_4)_2KMoO_3F_3$

Space group	a, Å	V, Å^3	2θ angle range, deg	Number of Bragg reflections	Number of refined parameters	R_p, %	R_{wp}, %	R_B, %
$Fm\bar{3}m$	9.0101(1)	731.45(1)	16.00–110.00	41	7	13.6	14.3	5.83

Note: a and V are the lattice parameter and unit cell volume, respectively; R_p, R_{wp}, and R_B are the profile, weighted profile, and Bragg confidence factors, respectively.

value of the pressure coefficient $(dT/dp)_{tr} \approx 300$ K/GPa; this coefficient decreases under pressure and becomes equal to 10 K/GPa at 0.6 GPa. The $Fm\bar{3}m \longrightarrow G_2$ phase transition line shown in Fig. 5a was measured only under a regime of increasing pressure, because hysteresis and relaxation phenomena were detected at pressures above p_{tr}.

Figure 5b shows the typical phase equilibrium curves obtained in several runs of measurements under a regime of a stepwise increase in pressure up to $p > p_{tr}$ followed by a decrease. It is seen that, beyond the tricritical point, there is a discrepancy between the data; as the pressure decreases, the interphase curve does not coincide with the curve measured under a regime of increasing pressure and, under $p < 0.2$ GPa, it approaches the equilibrium phase transition line (curves *1* and *2* in Fig. 5b). Thermal cycling experiments under pressures above the tricritical point were performed for a fixed value of the initial pressure (~0.35 GPa). In this case, a significant instability in the transition temperature was observed (curve *3* in Fig. 5b). After subsequent holding at this pressure for 15 h at room temperature, the phase transition was detected at the temperature corresponding to the equilibrium phase line. Then, the pressure was abruptly decreased to atmospheric pressure and a DTA anomaly appeared at ~246 K, which is 7 K above the equilibrium transition temperature. On repeated heating of the sample after holding at room temperature for 1 h, the transition temperature was measured to be 239 K, which corresponds to an equilibrium phase transition. The data on the heat capacity and the effect of pressure on the cubic phase stability made it possible to determine the region of existence of the metastable state in the crystal $(NH_4)_2KMoO_3F_3$ (shaded area in Fig. 5a).

Based on the results of heat capacity studies and the $p–T$ phase diagram of $(NH_4)_2KMoO_3F_3$, we can draw the following conclusion. Unlike in its tungsten analog, the phase transition from the cubic phase in this elpasolite can occur in relatively wide temperature and pressure ranges, depending on the prehistory of the measurements.

5. CRYSTAL STRUCTURE

To refine the structure of the cubic phase in $(NH_4)_2KMoO_3F_3$ using the Rietveld technique, the x-ray diffraction spectra of polycrystalline samples col-

lected on a D8-ADVANCE x-ray diffractometer (CuK$_\alpha$ radiation, θ–2θ scanning) were analyzed. The 2θ scanning step was 0.02° with 15-s exposure at each point. To decrease the effect of texture on the reflection intensity, the samples were rotated at a frequency of 0.5 s^{-1}.

The unit cell parameter was determined with the WTREOR program [7] and was refined during adjustment of the peak profiles of an x-ray powder pattern with the WINPLOTR program [8]. The basic parameters of data collection and structural refinement are listed in Table 1.

At the first stage, the unit cell parameter was refined and then the peak profiles were fitted.

At the second stage, the structure was refined. The coordinates of atoms in the isostructural compound $(NH_4)_2KMoO_3F_3$ [3] were taken for the refinement. A Mo atom substitutes for a W cation in the $4a$ position (0, 0, 0). Atoms O(F) (statistically disordered in the crystal) are in position (x, 0, 0) with a population of 0.5. The refined coordinate x is –0.2097(3). The thermal parameters of atoms Mo, K, and N were refined isotropically. The coordinates of atom H, which was at a distance of 0.8 Å from atom N, and the thermal parameter were not refined. The observed electron density in a section crossing the MoO_3F_3 octahedron is shown in Fig. 6. It is seen that the isolines do not correspond to concentric circles; therefore, the heat parameter of O(F) atoms was then refined in an anisotropic approach. Due to the cubic symmetry, only two components of the tensor of anisotropic oscillations should be refined instead of six. Thus, the parameters of anisotropic oscillations are $U_{11} = 0.0016(5)$ Å^2 and $U_{22} = U_{33} = 0.0303(6)$ Å^2. The results of refining the structure are shown in Table 1, and the coordinates of atoms, the thermal parameters,

Table 2. Coordinates of atoms in $(NH_4)_2KMoO_3F_3$, isotropic thermal parameters (B_{iso}), and position populations (p)

Atom	p	x	y	z	B_{iso}, Å^2
Mo	1.0	0	0	0	3.00(4)
K	1.0	0.5	0.5	0.5	4.33(8)
N	1.0	0.25	0.25	0.25	1.6(1)
H	1.0	0.198	0.198	0.198	1.0
F	0.5	0.2097(3)	0	0	6.74*
O	0.5	0.2097(3)	0	0	6.74*

* The thermal parameter was refined anisotropically.
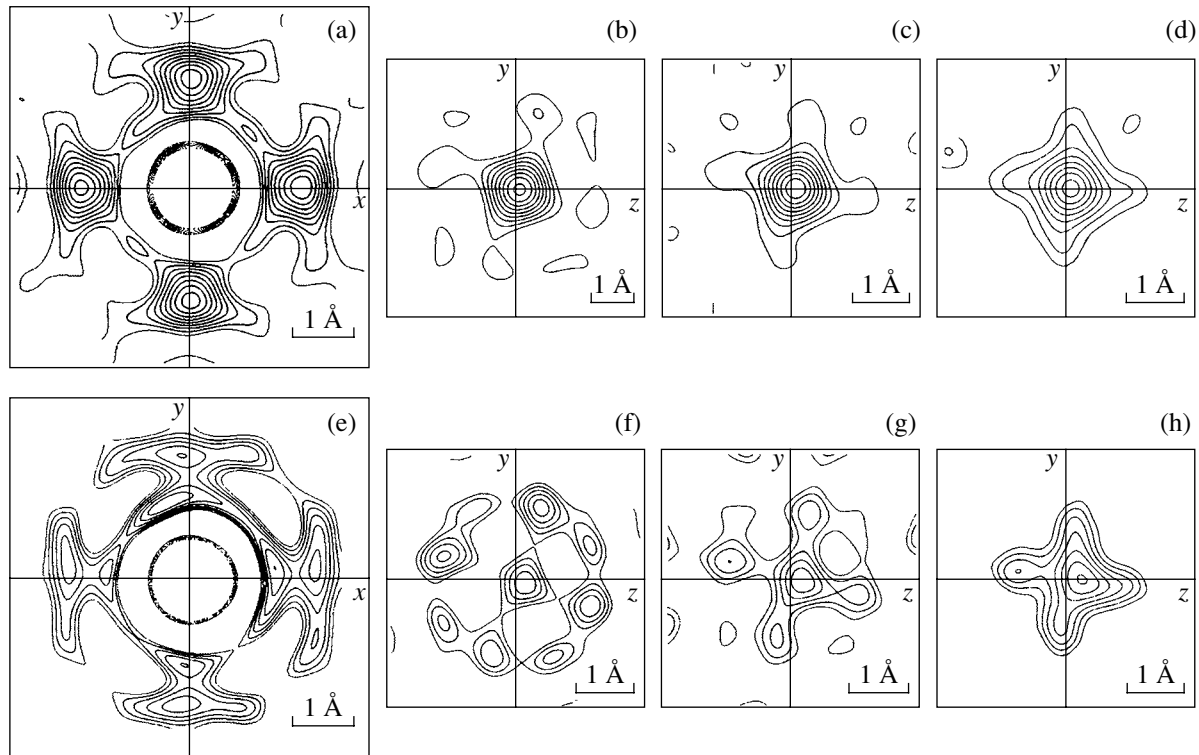
Fig. 6. Electron density maps (step 0.4 electron/$Å^3$) for (a–d) $(NH_4)_2KMoO_3F_3$ and (e–h) $(NH_4)_2KWO_3F_3$ [3]. (a, e) $z = 0$, (b, f) $x = 0.195$; (c, g) $x = 0.215$; and (d, h) $x = 0.235$.

and the populations of the positions are listed in Table 2.

In Fig. 6, several cross sections of the octahedron of the tungsten analog previously studied in [3] are shown. Apparently, a significant difference in the character of the density distribution exists in two compounds. This will be discussed below.

6. ANALYSIS OF THE EXPERIMENTAL RESULTS

We established that the elpasolite $(NH_4)_2MoO_3F_3$ has a cubic structure at room temperature. As the temperature decreases, it undergoes a single phase transition at $T_0 = 239$ K. The temperature of this transition is only ~45 K above the temperature of instability of the cubic phase of the isostructural tungsten compound, although according to studies of tungstates and molybdates with atomic cations [1] one might expect the transition temperature to be several tens of kelvins higher. Thus, it is unlikely that the idea expressed in [6] of there being a significant influence of the covalency of the M–O bond on the temperature of the structural transition from the cubic phase can be applied in the case of structures containing a tetrahedral cation.

On the other hand, the substitution W $\longrightarrow$ Mo leads to a first-order transition in the elpasolite $(NH_4)_2KMoO_3F_3$ under atmospheric pressure. This is confirmed by the hysteresis in the transition tempera-

ture, the jump in the unit cell parameters, and the latent heat of the phase transition. Moreover, the ratio between the latent heat and total change in enthalpy $\delta H/\Delta H = 0.7$ is high enough to show that this transition is rather far from the tricritical point.

The relative jump in the unit cell volume of $(NH_4)_2KMoO_3F_3$ at the phase transition point was determined from the unit cell parameters $a_i(T)$ to be $\delta V/V = -0.24\%$. The volume jump was also calculated from the Clapeyron-Clausius equation based on the data on the shift in the transition temperature and entropy jump under pressure determined in this work and was found to be −23%. The good coincidence of the values of $\delta V/V$ found by independent measurements confirms the reliability of the experimental results.

The studies of the phase diagram revealed that the ΔS values corresponding to the phase transitions from the cubic phase are the same over the entire pressure range studied Therefore, the difference between the values of dT/dp at the $Fm\bar{3}m \longrightarrow G_1$ and $Fm\bar{3}m \longrightarrow G_2$ phase transition lines is caused by the change in the value and sign of the volume jump. The fact that dT_0/dp does not change up to the tricritical point means that the degree of proximity of this transition to the tricritical point remains unchanged. The abrupt change in dT/dp under pressures above p_{tr} indicates that there is an anomalous change in the sign and value of the volume

jump at the tricritical point due to a change in the ratios between the jumps in the lattice parameters. The decrease in *dT/dp* without a change in ΔS over this pressure range means that the volume jump decreases as the pressure increases; i.e., the transition approaches the tricritical point.

When studying the temperature dependence of the heat capacity of $(NH_4)_2KMoO_3F_3$, we observed hysteresis and relaxation effects, which were manifested in the dependence of the temperature of the maximum excess heat capacity ΔC_p (the phase transition temperature) on the prehistory of a specific run of measurements. It was established that it is possible to transfer the system to a stable state by annealing at room temperature over 10–15 h. Similar phenomena were also observed in the studies of the *p–T* phase diagram. These circumstances could be explained by the fact that the phase transition in question is found to be far from the tricritical point, because in this case a wide range of instable states exist in the *p–T* diagram of the system studied.

It should be noted that studies of the cryolite $(NH_4)_2NH_4WO_3F_3$ under pressure [2], in which the phase transition is likewise far from the tricritical point $(\delta S_0/\Delta S = 0.8)$, have shown that this compound has a similar phase diagram. However, on the one hand, both boundaries of the range of existence of the high-pressure phase were reliably determined by the DTA technique under $p > p_{tr}$. The transition into this phase from the cubic phase was characterized by a far smaller entropy ($R \ln 2$) than the $G_2 \longrightarrow G_1$ transition ($R \ln 4$). On the other hand, the relaxation phenomena indicated above were not observed in the calorimetric and DTA experiments under pressure.

It can be expected that the features mentioned above in the behavior of the thermophysical properties of $(NH_4)_2KMoO_3F_3$ should manifest themselves in the mechanism of the phase transition. It was established experimentally that this transition is characterized by a significant change in entropy ($\Delta S_0 = 13.0 \pm 0.7$ J/mol K = $1.56R = R \ln 4.8$) and, thus, is of the order–disorder type. According to the model of disorder in the cubic phase of ammonium elpasolite [3], the entropy of the phase transition can be caused by an ordering of octahedrons MO_3F_3 and tetrahedrons NH_4. However, from an analysis of the electron density maps, it follows that, though atoms F(O) in $(NH_4)_2KMoO_3F_3$ (Fig. 6) vibrate anisotropically, they are located on a unit cell edge, on the average, with a higher probability than in the related compounds $(NH_4)_2KWO_3F_3$ and $(NH_4)_2NH_4WO_3F_3$ [3]; consequently, they cannot contribute significantly to the entropy of the transition. However, a comparison of the thermal parameters of atoms F(O) shows the opposite.

The quantity B_{iso} in molybdenum elpasolite (Table 2) is approximately 2.5 times higher than that in the tung-

sten analog ($\Delta S_0 = R \ln 1.8$) [3] and is close to the thermal parameter of atoms F(O) in $(NH_4)_2NH_4WO_3F_3$ (6.5 Å^2) [3], which undergoes an order–disorder transition ($\Delta S_0 = R\ln 8$). Another special feature of molybdenum elpasolite is that the thermal parameters of molybdenum and potassium atoms are significantly higher than those in the tungsten compounds [3]. It can be assumed that these atoms are likewise involved in the phase transition and that the structural features of the molybdate mentioned above cause a difference in its thermophysical properties.

In view of the above discussion, the question as to the role played by the ammonium groups in the structural distortion still remains open and studies of the proton subsystem in both tungstate and molybdate are of interest.

REFERENCES

1. J. Ravez, G. Peraudeau, H. Arend, S. C. Abrahams, and P. Hagenmüller, Ferroelectrics **26**, 767 (1980).

2. I. N. Flerov, M. V. Gorev, V. D. Fokina, A. F. Bovina, and N. M. Laptash, Fiz. Tverd. Tela (St. Petersburg) **46** (5), 888 (2004) [Phys. Solid State **46** (5), 915 (2004)].

3. I. N. Flerov, M. V. Gorev, V. D. Fokina, A. F. Bovina, M. S. Molokeev, Yu. V. Boĭko, V. N. Voronov, and A. G. Kocharova, Fiz. Tverd. Tela (St. Petersburg) **48** (1), 99 (2006) [Phys. Solid State **48** (1), 106 (2006)].

4. A. Tressaud, S. Khairoun, L. Rabardel, T. Kobayashi, T. Matsuo, and H. Suga, Phys. Status Solidi A **96**, 407 (1986).

5. I. N. Flerov, M. V. Gorev, K. S. Aleksandrov, A. Tressaud, and V. D. Fokina, Kristallografiya **49** (1), 107 (2004) [Crystallogr. Rep. **49** (1), 100 (2004)].

6. G. Peraudeau, J. Ravez, P. Hagenmüller, and H. Arend, Solid State Commun. **27**, 591 (1978).

7. P.-E. Werner, L. Eriksson, and M. Westdahl, J. Appl. Crystallogr. **18**, 367 (1985).

8. T. Roisnel and J. Rodrigues-Carvajal, in *Proceedings of the European Powder Diffraction Conference "EPDIC7," Barcelona, Spain, 2000* (Mater. Sci. Forum, 2000), Vols. 378–381, Parts 1–2, p. 118.

Translated by E. Borisenko